# Development and Validation of a New In-Situ Technique to Measure Total Gaseous Chlorine in ~~Ambient~~ Air

Teles C. Furlani[1], RenXi Ye[1], Jordan Stewart[1,2], Leigh R. Crilley[1], Peter M. Edwards[2], Tara F. Kahan[3], Cora J. Young[1*]

[1] Department of Chemistry, York University, Toronto, Canada

[2] Department of Chemistry, University of York, York, UK

[3] Department of Chemistry, University of Saskatchewan, Saskatoon, Canada

*Correspondence to: youngcj@yorku.ca

**Abstract**

Total gaseous chlorine ($TCl_g$) measurements can improve our understanding of unknown sources of Cl to the atmosphere. Existing techniques for measuring $TCl_g$ have been limited to offline analysis of extracted filters and do not provide suitable temporal information on fast atmospheric process. We describe high time-resolution in-situ measurements of $TCl_g$ by ~~combusting~~ thermolyzing ~~ambient~~ air over a heated platinum (Pt) substrate coupled to a cavity ring-down spectrometer (CRDS). The method relies on the complete decomposition of $TCl_g$ to release Cl atoms that react to form HCl, for which detection by CRDS has previously been shown to be fast and reliable. The method was validated using custom organochlorine permeation devices (PDs) that generated gas-phase dichloromethane (DCM), 1-chlorobutane (CB), and 1,3-dichloropropene (DCP). The optimal conversion temperature and residence time through the high-temperature furnace was 825 °C and 1.5 seconds, respectively. Complete conversion was observed for six organochlorine compounds, including alkyl, allyl, and aryl C-Cl bonds, which are amongst the strongest Cl-containing bonds. ~~of gravimetrically validated PDs was indicated by the near unity~~

26 ~~orthogonal distance regression analysis slope (±σ) of~~ measured $TCl_g$ plotted against expected $TCl_g$

27 ~~and was~~ 0.996 ± 0.012, 1.048 ± 0.0060, and 1.027 ± 0.061 for DCM, CB, and DCP, respectively.

28 The quantitative conversion of these strong C-Cl bonds suggests complete conversion~~Breaking~~

29 ~~these relatively strong C-Cl bonds represents a proof of concept for complete conversion~~ of ~~all~~

30 similar or weaker bonds that characterize all other $TCl_g$. We applied this technique to both outdoor

31 and indoor environments and found reasonable ~~comparisons~~ agreements in ambient background

32 mixing ratios with the sum of expected HCl from known long-lived Cl species. We measured the

33 converted $TCl_g$ in an indoor environment during cleaning activities and observed varying levels of

34 $TCl_g$ comparable to previous studies. The method validated here is capable of measuring in-situ

35 $TCl_g$ and has a broad range of potential applications ~~to make routine $TCl_g$ measurements in a~~

36 ~~variety of applications~~.

## 1. Introduction

38        Chlorine (Cl) containing compounds in the atmosphere can impact air quality, climate, and

39 health (Saiz-Lopez and Von Glasow, 2012; Simpson et al., 2015; Massin et al., 1998; White and

40 Martin, 2010). Gaseous chlorinated compounds are either organic (e.g., dichloromethane,

41 chloroform, and carbon tetrachloride) or inorganic (e.g., $Cl_2$, HCl, and $ClNO_2$), with inorganic

42 ~~chlorine~~ Cl being more reactive under most atmospheric conditions. In this work, total gaseous

43 ~~chlorine~~ Cl ($TCl_g$) refers to all gas-phase ~~chlorine~~Cl-containing species weighted to their Cl

44 content, including both inorganic and organic species. While groups of chlorinated species are

45 often considered based on reactivity considerations (e.g., reactive chlorine, $Cl_y$), $TCl_g$ includes all

46 molecules that contain one or more Cl atoms:

47 $TCl_g = 4*[CCl_4] + 3*[CHCl_3] + 2*[CH_2Cl_2] + [CH_3Cl] + 2*[Cl_2] + [HOCl] + \ldots\ldots$        E1

48   Impacts on air quality and climate are due to the high reactivity of atomic Cl produced by common

49   atmospheric reactions (e.g., photolysis and oxidation) of Cl-containing compounds (Haskins et al.,

50   2018; Riedel et al., 2014; Sherwen et al., 2016). The Cl cycle is important to atmospheric

51   composition in the stratosphere and troposphere, affecting species including methane, ozone, and

52   particles (both formation and composition), which influence air quality and climate (Solomon,

53   1999; Riedel et al., 2014; Young et al., 2014; Sherwen et al., 2016). High levels of some $TCl_g$

54   species (e.g., $Cl_2$ and carbon tetrachloride) are known to be toxic (White and Martin, 2010; Unsal

55   et al., 2021). The implications of many $TCl_g$ species on human health are not well understood for

56   low level exposure for extended periods of time. Potential health impacts of organic chlorinated

57   compounds include hepatotoxicity, nephrotoxicity, and genotoxicity (Unsal et al., 2021;

58   Henschler, 1994). Impacts of inorganic chlorinated species include the chlorination of squalene, a

59   major part of human skin oils, by HOCl (Schwartz-Narbonne et al., 2019); respiratory irritation

60   and airway obstruction by $Cl_2$ (White and Martin, 2010); and increased incidence of asthma and

61   other chronic respiratory issues following exposure to chloramines (Massin et al., 1998).

62      Sources of Cl to the atmosphere are highly variable and depend on both direct emissions

63   and indirect regional Cl activation chemistry (Finlayson-Pitts, 1993; Raff et al., 2009; Khalil et al.,

64   1999). Direct emissions of $TCl_g$ can come from numerous natural and anthropogenic activities

65   such as, but not limited to, ocean and volcanic emissions, biomass burning, disinfection (i.e.,

66   household cleaning, pool emission, etc), use of solvents and heat transfer coolants, and incineration

67   of chlorinated wastes (Blankenship et al., 1994; Lobert et al., 1999; Keene et al., 1999; Butz et al.,

68   2017; Wong et al., 2017; Fernando et al., 2014). Activation of Cl is another source, occurring when

69   atmospheric processes transform relatively unreactive chloride ($Cl^-$, such as sea salt, NaCl) into

70   reactive gaseous chlorine ($Cl_y$), which will contribute to $TCl_g$. Understanding global levels of $TCl_g$

71 is difficult due to complex emissions and chemistry. Our best estimates come from modelling

72 studies combined with collaborative efforts to compose policy reports on halogenated substances,

73 such as the World Meteorological Organization (WMO) Scientific Assessment of Stratospheric

74 Ozone Depletion (WMO (World Meteorological Organization), 2018). Mixing ratio estimates of

75 halogenated species from this report are summed from individual measurements (e.g., National

76 Oceanic and Atmospheric Administration (NOAA) and Advanced Global Atmospheric Gases

77 Experiment (AGAGE)). The WMO report includes flask (captured gas from clean air sectors) and

78 in-situ measurements from field campaigns and routine sampling sites (e.g., CONvective

79 Transport of Active Species in the Tropics (CONTRAST)) (Prinn et al., 2018; Pan et al., 2017;

80 Andrews et al., 2016; Montzka et al., 2021; Adcock et al., 2018). In the most recent WMO report

81 (2018), a decrease of $12.7 \pm 0.9$ pptv Cl yr$^{-1}$ in total tropospheric Cl was determined for Montreal

82 Protocol-controlled substances (e.g., chlorofluorocarbons (CFCs) and hydrochlorofluorocarbons

83 (HCFCs)). The decrease in Montreal Protocol-controlled emissions has been slightly offset by an

84 increase in relatively short-lived substances (e.g., dichloromethane) that are not controlled by the

85 Montreal Protocol (WMO (World Meteorological Organization), 2018). Despite the emissions of

86 these regulated chlorinated species being relatively well-constrained, new sources for some of

87 these compounds have appeared in the recent past. For example, unexpected increases observed in

88 CFC-11 emissions suggested new unreported production (WMO (World Meteorological

89 Organization), 2018). A new source of chloroform was also recently identified and attributed to

90 halide containing organic matter derived from penguin excrement in the Antarctic tundra (Zhang

91 et al., 2021). Atmospheric levels of TCl$_g$ will additionally be impacted by emission sources that

92 are relatively poorly constrained, including combustion and disinfection. Increasing levels of

93 chlorinated species from known and unknown pathways was observed in a recent ice core study,

94    which estimated an increase of up to 170% of $Cl_y$ (= BrCl + HCl + Cl + ClO + HOCl + $ClNO_3$ +

95    $ClNO_2$ + ClOO + OClO + $2 \cdot Cl_2$ + $2 \cdot Cl_2O_2$ + ICl) from preindustrial times to the 1970s could be

96    attributed to mostly anthropogenic sources (Zhai et al., 2021).

97    Understanding $TCl_g$ source and sink chemistry is not only important for the ambient

98    atmosphere but also for indoor environments. Uncertainty in sources and levels of chemicals,

99    including chlorine-containing compounds, indoors is related to heterogeneity in sources and

100    individual indoor environments, and the fact that relatively few studies have focused on indoor

101    chemistry compared to outdoor. The role of chlorinated species on indoor air quality has been

102    investigated in a few studies (Mattila et al., 2020; Wong et al., 2017; Dawe et al., 2019; Giardino

103    and Andelman, 1996; Shepherd et al., 1996; Doucette et al., 2018; Nuckols et al., 2005). Most

104    studies have focused on cleaning with chlorine-based cleaners, in which HOCl and other inorganic

105    compounds have been observed in the gas phase at high levels (Wong et al., 2017; Wang et al.,

106    2019; Mattila et al., 2020). Some studies have reported the presence of organic chlorinated species

107    such as chloroform and carbon tetrachloride above bleach cleaning solutions indoors (Odabasi,

108    2008; Odabasi et al., 2014), and chloroform has been observed during water-based cleaning

109    activities, such as showering and clothing washing (Nuckols et al., 2005; Shepherd et al., 1996;

110    Giardino and Andelman, 1996).

111    Constraining the Cl budget is critical to better understanding its contributions to climate,

112    air quality, and human health. Robust total Cl measurements are useful because it is not always

113    feasible to routinely deploy individual measurements of the large number of Cl-containing

114    compounds (Table S1). As described above, estimates of $TCl_g$ from models and summed

115    measurements have demonstrated gaps in our knowledge. It is therefore essential to have a method

116    capable of measuring true $TCl_g$ to explain discrepancies between model and measured estimates

117  due to unknown species. Measurements of total elemental composition in the condensed phase,

118  including total Cl, have been used for monitoring and managing both known and unknown

119  compounds (Miyake et al., 2007c, a; Yeung et al., 2008; Miyake et al., 2007b; Kannan et al., 1999;

120  Xu et al., 2003; Kawano et al., 2007). However, $TCl_g$ methods have been limited to offline analysis

121  of scrubbed sample gas (e.g., flue); these methods rely on multiple extraction steps and the

122  application of condensed-phase total Cl analyses, such as combustion ion chromatography

123  (Miyake et al., 2007a; Kato et al., 2000) or neutron activation analysis (Berg et al., 1980; Xu et al.,

124  2006, 2007). Because offline techniques suffer from extraction uncertainties and do not have the

125  temporal resolution to effectively probe fast ~~source and sink~~ chemistry in the atmosphere, in-situ

126  measurements of total elemental gaseous composition have been developed for several elements

127  (Hardy and Knarr, 1982; Veres et al., 2010; Roberts et al., 1998; Maris et al., 2003; Yang and

128  Fleming, 2019). For example, total nitrogen has been measured using Pt-catalyzed thermolysis

129  coupled to online chemiluminescence detection (Stockwell et al., 2018). Using a similar approach,

130  we describe here a method for $TCl_g$, where catalyzed thermolysis is coupled to a high time-

131  resolution HCl cavity ring-down spectrometer (CRDS). This technique relies on the complete

132  thermolysis of $TCl_g$, which yields chlorine atoms. These Cl atoms readily form HCl via hydrogen

133  abstraction (R1), in this case from propane (or its thermolysis products) that is supplied in excess.

$$Cl\ (g) + C_3H_8\ (g) \rightarrow HCl\ (g) + C_3H_7\ (g) \hspace{3cm} R1$$
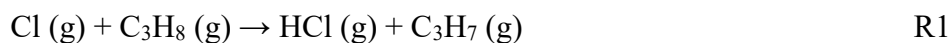
134      The objectives of this paper are to: (i) Develop and validate an instrument capable of in-

135  situ measurement of $TCl_g$ through conversion to HCl and detection by CRDS; and (ii) demonstrate

136  application of the technique to outdoor and indoor $TCl_g$ measurements.

## 2. Materials and experimental methods

### 2.1. Chemicals

Commercially available reagents were purchased from Sigma-Aldrich (Oakville, Ontario, Canada): dichloromethane (DCM, HPLC grade, ~~Oakville, Ontario, Canada~~), 1-chlorobutane (CB, 99.5%, ~~Milwaukee, Wisconsin, USA~~), cis-1,3-dichloropropene (DCP, 97%, ~~Milwaukee, Wisconsin, USA~~), trichlorobenzene (TrCB, 99%), tetrachlorobenzene (TeCB, 98%), pentachlorobenzene (PeCB, 96 %), sodium chloride, and 52 mesh sized platinum catalyst (99.9 %, ~~Milwaukee, Wisconsin, USA~~). Toluene (HPLC grade) was purchased from BDH VWR (Mississauga, Ontario, Canada). Nitrogen (grade 4.8) and propane ($C_3H_8$, 12.7% in nitrogen, v/v) gas was from Praxair (Toronto, Ontario, Canada). Experiments used deionized water generated by a Barnstead Infinity Ultrapure Water System (Thermo Fisher Scientific, Waltham, Massachusetts, USA; 18.2 MΩ cm$^{-1}$). A permeation device (PD) described previously was used to generate gaseous HCl (Furlani et al., 2021). Chlorine-free~~lean~~ zero air was generated by a custom-made zero-air generator.

### 2.2. HCl and total chlorine (HCl-TCl) instrument

The main components of the HCl-TCl (Figure 1) are platinum catalyst mesh, a quartz glass flow tube, a split-tube furnace (Protégé Compact, 1100°C max temperature, Thermcraft incorporated, North Carolina, USA), and a CRDS HCl analyzer (Picarro G2108 Hydrogen Chloride Gas Analyzer). The platinum catalyst consisted of ~2 g platinum mesh with a total combined surface area of 134 cm$^2$. Sample gas was mixed with critical orifice-regulated (Lenox laser, Glen Arm, Maryland, USA, 30 psi; SS-4-VCR-2-50) propane gas (62 ± 6 standard cubic centimetres per minute (sccm)), provided in excess prior to introduction to the furnace to promote (R1). The added ~~P~~propane does not fully ~~combust~~ thermolyze at temperatures < 650 °C, which can lead to spectral interferences in the CRDS analyzer (Figure S1) and should only be added when

161 temperatures exceed 650°C (Furlani et al., 2021). All lines and fittings were made of

162 perfluoroalkoxy (PFA) unless stated otherwise. The mixing line carrying clean air dilution flows

163 was controlled by a 10 L min$^{-1}$ mass flow controller (MFC, GM50A, MKS instruments, Andover,

164 Massachusetts, USA). The length of the sample gas tubing to the furnace was 0.6 m, and the

165 transfer line between the furnace and CRDS was 0.2 m. The furnace transfer line met an overflow

166 tee when delivering flows greater than the CRDS flowrate of 2 L min$^{-1}$. The coupled CRDS can

167 capture transient fast HCl formation processes on the timescale of a few minutes, limited by the

168 high adsorption activity of HCl on inlet surfaces (discussed further in Section 3.3) effects. The

169 CRDS collects data at 0.5 Hz, which was averaged to 30 sec for the purposes of this work. Limits

170 of detection (LODs) for the CRDS were calculated as three times the Allan–Werle deviation in

171 raw signal intensity when overflowing the inlet with zero air directed into the CRDS for ~ 10 h.

172 The 30-sec limit of detection (LOD) is 18 pptv and well below expected HCl from TCl$_g$ conversion

173 (Furlani et al., 2021).

174



175
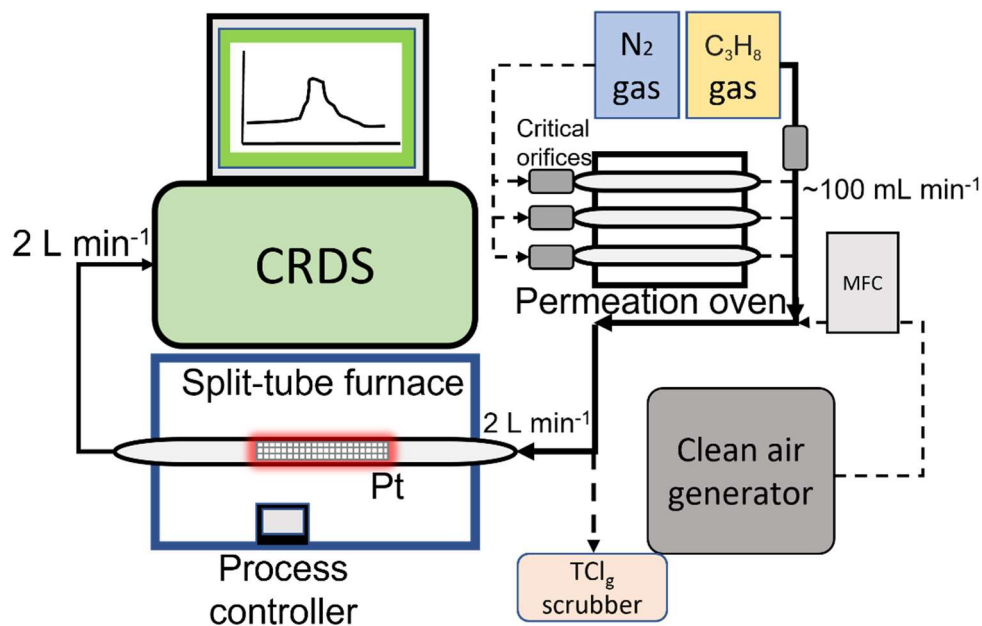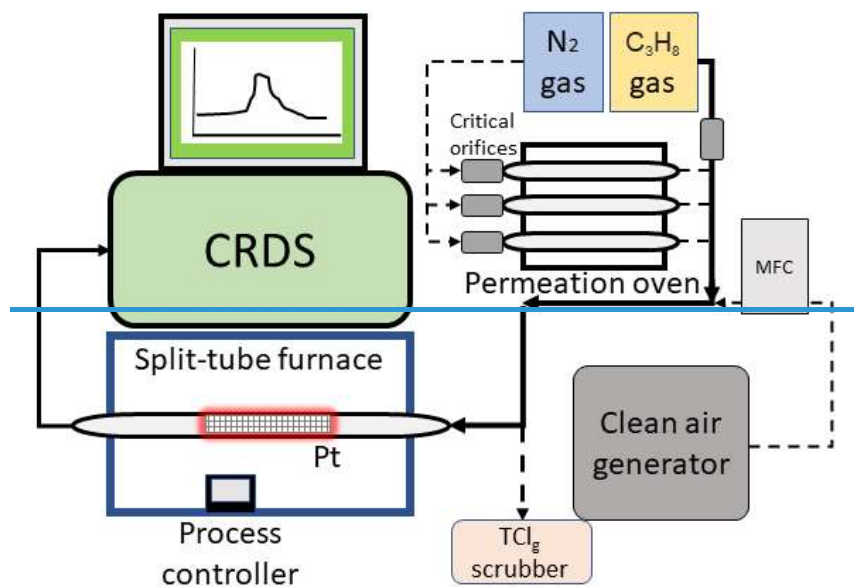
**Figure 1.** Sampling schematic showing the key components of the HCl-TCl coupled to the CRDS analyzer. Dashed lines indicate parts of the apparatus used only during validation. Not to scale.

**2.3.   Preparation of <u>organochlorine</u> permeation devices (PDs)**

<u>Organochlorine</u> ~~Permeation devices (~~PDs~~)~~ were prepared as follows: approximately 200 μL

of DCM, CB, or DCP was pipetted into a 50 mm PFA tube (3 mm i.d. with 1 mm thickness),

thermally sealed at one end and plugged at the other end with porous polytetrafluoroethylene

182 (PTFE) (13 mm length by 3.17 mm o.d.). The polymers allow a consistent mass of standard gas to

183 permeate at a given temperature and pressure. The method for temperature and flow control of the

184 PDs is described in detail in Lao et al. (2020). Briefly, an aluminum block that was temperature-

185 controlled (Omega$^{TM}$; CN 7823, Saint-Eustache, QC, Canada) using a cartridge heater (Omega$^{TM}$;

186 CIR-2081/120V, Saint-Eustache, QC, Canada) housed the PD and was regulated to $30.0 \pm 0.1$ °C.

187 Dry $N_2$ gas flowed through a PFA housing tube (1.27 cm o.d.) in the block that contained the PD.

188 Stable flows of carrier gases passed through the housing tube in the oven were achieved using a

189 50 μm diameter critical orifice (Lenox laser, Glen Arm, Maryland, USA, 30 psi; SS-4-VCR-2-50)

190 and were $120 \pm 12$, $99 \pm 9.9$ and $120 \pm 12$ sccm for DCM, CB, and DCP, respectively. Flows were

191 measured using a DryCal Definer 220 (Mesa Labs, Lakewood, Colorado, USA). The mass

192 emission rate of each organochlorine from the PDs was quantified gravimetrically ov~~Fig~~er a period

193 of approximately 4 weeks (mass accuracy $\pm$ 0.001 g). Mass emission rates for each PD were

194 determined as $640 \pm 10$, $240 \pm 40$, and $1.20 \times 10^4 \pm 0.02 \times 10^4$ ng min$^{-1}$ (n=3, $\pm$ 1σ) at 30 °C for

195 DCM, CB, and DCP, respectively.

196 **2.4. HCl-TCl optimization**

197 Gas phase standards of DCM, CB, and DCP were used to test the conversion efficiency of

198 chlorinated compounds to form HCl. Bond dissociation energies for carbon-Cl bonds typically

199 range between 310 and 410 kJ mol$^{-1}$ (Tables S1, S2). The split-tube furnace has a process controller

200 capable of increasing or decreasing temperature at a set °C min$^{-1}$, which allowed us to identify the

201 temperature at which enough energy was provided to break the bonds. By introducing a consistent

202 amount of each of the organochlorines, separately, to the HCl-TCl set over a simple temperature

203 ramping program we could monitor in real-time the conditions necessary to break the bonds by

204 measuring the formation of the resulting HCl. The ~~conversion~~ operating temperature was

205 determined when complete conversion of the measured TCl$_g$ for the tested compounds when the

206 measured HCl plateaued and was sustained at 100% conversion based on PD emission rates.

207       To determine the optimal residence time in the quartz tube with the Pt catalyst, flows of

208 0.6–5.5 L min$^{-1}$ containing DCM sample gas in clean air were tested yielding a range of residence

209 times between 0.5 and 4.5 sec in the furnace. Temperature remained constant at 825 °C throughout

210 the experiment, and a dilution flow of 4.0 L min$^{-1}$ of clean air was added to the sample flow exiting

211 the furnace before introduction to the CRDS.

212       We tested the HCl transmission of the HCl-TCl at 2 mixing ratios (18 and 10 ppbv) using

213 a 12 M HCl PD with zero air dilution flows of 3.5 or 5 L min$^{-1}$ using a 5 L min$^{-1}$ MFC (GM50A,

214 MKS instruments, Andover, Massachusetts, USA). The HCl recovery through the furnace was

215 tested by comparing measured HCl mixing ratios through HCl-TCl to those with the furnace flow

216 tube replaced by a similar length of tubing. A heat gun (Master Varitemp® vt-750c) was used to

217 heat the flow tube entrance to ~80 °C to minimize HCl sorption. We tested the HCl-TCl conversion

218 efficiency for 5 different mixing ratios of three organochlorine PD standards (DCM, CB, and DCP)

219 under three conditions: (1) both Pt catalyst and added propane, (2) only Pt catalyst, and (3) only

220 added propane. Each gas was tested individually under the same conditions; sample gas from PDs

221 was mixed with propane and immediately diluted into clean air using a 10 L min$^{-1}$ MFC (GM50A,

222 MKS instruments, Andover, Massachusetts, USA). The dilution flows ranged from 2.2–9.0 L min$^{-1}$

223 $^{1}$. The sampling lines were the same lengths as stated previously. In this experiment, the CRDS

224 flowrate of 2 L min$^{-1}$ was sufficient to give an optimal residence time of 1.5 sec through the HCl-

225 TCl (see Section 3.1). In all experiments the CRDS subsampled through the furnace from the main

226 transfer line and the excess gas was directed outdoors through a waste line containing a carbon

227 trap (Purakol, Purafil, Inc, Doraville, Georgia, USA). We tested the HCl-TCl conversion efficiency

for two different quantities of three chlorobenzenes (TrCB, TeCB, and PeCB). Due to their high boiling points, PDs of these compounds could not be prepared. Instead, small volumes of approximately 1 mM solutions of these compounds dissolved in toluene were directly introduced to the HCl-TCl while it was sampling room air. oom air measurements of $TCl_g$ were consistently >1 ppbv. These were measured before each experiment and did not affect the peak integration described below. With a short piece of tubing used as an inlet, 1 and 2 μL of each compound was injected onto the inner surface of the tubing, which was heated to ~100 °C with a heat gun to facilitate volatilization. The resulting signals were integrated over a time period of 2.5 hours to obtain the total quantity of HCl detected by the CRDS, which was used to calculate conversion efficiency. To account for uncertainties in peak integration, a high and low peak area boundary was determined, with the average peak area taken for each injection. Duplicates of each injected quantity were performed, except for 1 μL TrCB, which was performed in triplicate.

To determine if there was any positive bias in the $TCl_g$, measurement from the conversion of particulate chloride ($pCl^-$), NaCl aerosols were generated by flowing 2 L min−1 of chlorine free zero air through a nebulizer containing a solution of 2% w/w NaCl in deionized water. The aerosol flow was then mixed with 1 L min$^{-1}$ of chlorine free dry zero air to achieve a total flow of 3 L min$^{-1}$, The HCl-TCl (2 L min$^{-1}$) then sampled off this main mixing line. Chloride was added after monitoring background zero air levels. After ~3 hours of measuring the converted $pCl^-$, a PTFE filter (2 μm pore size, 47 mm diameter, TISCH scientific, North Bend, Ohio, USA) was added inline onto the inlet of the HCl-TCl.

**2.5. Outdoor air HCl-TCl measurements**

Outdoor air sampling was performed betweenon 00:00 on July 7 to 20:00 on July 11, August 6 and November 17–19, 2021 2022 (Eastern daylight time, EDT). The sampling site was the air

251  quality research station located on the roof of the Petrie Science and Engineering building at York

252  University in Toronto, Ontario, Canada (43.7738° N, 79.5071° W, 220 m above sea level). The

253  HCl-TCl was co-located with a Campbell scientific weather station paired with a cr300 datalogger.

254  All inlet lines and fittings were made of PFA unless stated otherwise. All indoor inlet lines and

255  fittings were kept at room temperature (20 to 25 °C) while outdoor temperatures ranged from 25

256  to 28 °C on August 6, and 0 to 17 °C in November. A mass flow controller (GM50A, MKS

257  instruments, Andover, Massachusetts, USA) regulated a sampling flow of 14.7 L min$^{-1}$ using a

258  diaphragm pump through a 2.4 m sampling inlet (I.D. of 0.375") from outdoors. The outdoor air

259  was pulled through a 2.5 μm particulate matter cut-off URG Teflon Coated Aluminum Cyclone

260  (URG Corporation, Chapel Hill, North Carolina, USA) with a 2.5 μm particulate matter cut-off to

261  remove the larger particles and then passed through a PTFE filter (2 μm pore size, 47 mm diameter,

262  TISCH scientific, North Bend, Ohio, USA). The CRDS subsampled 2 L min$^{-1}$ through the furnace

263  off the main inlet line, yielding a total inlet flow of 16.7 L min$^{-1}$. The apparatus had zero air

264  overflow the inlet 1 hour prior to and after outdoor sampling. The CRDS sample flow passed first

265  through a PTFE filter (2 μm pore size, 47 mm diameter, TISCH scientific, North Bend, Ohio,

266  USA) and then two high efficiency particulate air (HEPA) filters contained within the CRDS outer

267  cavity metal compartment heat-regulated to 45 °C. Instances of flagged instrument errors in the

268  CRDS data during ambient observations were removed as standard practice in quality control

269  procedures (Furlani et al., 2021).

270  **2.6.   Indoor air HCl-TCl and HOCl analyzer measurements**

271       To test indoor applications of the HCl-TCl, a 1 m$^2$ area of laboratory floor was cleaned with

272  a commercial spray bottle cleaner (1.84 % sodium hypochlorite w/w) and emissions were

273  compared with an HOCl analyzer. The HOCl analyzer is a commercial instrument designed to

274  quantify gaseous hydrogen peroxide ($H_2O_2$) using CRDS (Picarro PI2114 Hydrogen Peroxide

275  Analyzer; Picarro Inc.). The instrument is also sensitive to HOCl due to similar absorbance

276  wavelengths of their first overtone stretches in the near IR. The wavelengths monitored have been

277  altered to selectively detect HOCl. Details on instrument calibration and validation are provided

278  in Stubbs et al. (2022) [Stubbs et al., in prep].

279      The distance from the suspended 2 m inlet lines of both instruments to the floor was ~1 m.

280  The flowrate through the furnace and inlet was the 2 L min$^{-1}$ CRDS flowrate. The flowrate for the

281  HOCl analyzer was 1 L min$^{-1}$. The sectioned off area was cleaned four times, spraying 32 times

282  for each application using the commercial cleaner. Three of these events were measured using the

283  HCl-TCl and HOCl analyzer, while one event was measured using the HCl CRDS only.

284  **3. Results and Discussion**

285  **3.1.  HCl-TCl temperature and residence time optimization**

286      We validated this method by testing conversion efficiency of organochlorines under different

287  operating parameters and conditions. Testing all TCl$_g$ species is not feasible, but by testing

288  compounds that contain strong Cl-containing bonds, we infer at least equal efficacy of the system

289  in the breakage of relatively weaker Cl-containing bonds (Tables S1 and S2). We selected very

290  strong Cl-containing bonds (i.e., alkyl, allyl, and aryl chlorides) and used them as a proxy for

291  compounds containing weaker Cl bonds; therefore, by demonstrating their complete conversion

292  we set precedent for conversion of all TCl$_g$. The temperature of the furnace is a key factor in

293  accomplishing complete thermolysis, and the minimum temperature of the furnace containing the

294  Pt catalyst to break the C-Cl bonds in DCM was determined. A simple temperature ramping

295  program was used to determine the breakthrough temperature. The temperature was increased at a

296  rate of 2.7 °C min$^{-1}$ starting at 300 °C and ending at 800 °C. The temperature breakthrough was

297    observed when complete conversion of the expected HCl for the tested compounds (based on PD

298    emission rate) was stable after reaching the optimal temperature. It was found to be ~800 °C for

299    the tested organochlorines (Figure S2).

300        Determining the optimal residence time of sample gas in the HCl-TCl is also essential for

301    an optimized $TCl_g$ conversion method. Using a temperature slightly above the observed

302    breakthrough temperature of 800 °C determined above (825 °C), six residence times were tested

303    with DCM, ranging from 0.5 to 4.5 seconds in the HCl-TCl (Figure 2Figure 2). At each residence

304    time the conversion efficiency was determined, where conversion efficiency was calculated as

305    follows:

306    $$\text{Conversion efficiency} = \frac{\text{Measured } TCl_g}{\text{Expected } TCl_g} \times 100 \text{ \%} \qquad \qquad \text{E}21$$

307    The optimal residence time was ~1.5 seconds, corresponding to a conversion efficiency of 100.1

308    ± 0.1 %. The uncertainty in conversion efficiency measurements is the variability in the measured

309    HCl signal for 30 minutes after a signal plateau was observed. The reported uncertainty does not

310    include uncertainties in mixing, or turbulence induced surface effects, which we cannot quantify.

311    When residence times were lower (i.e., sample gas traveled more quickly through the system) than

312    1.5 seconds, the conversion efficiencies were lower by 2 – 10 %, the measured HCl signal was

313    more erratic, and it took longer to stabilize. When residence times were higher (i.e., sample gas

314    traveled more slowly through the system) than 1.5 seconds, the conversion efficiencies were

315    comparable (± 2 %), but the measured HCl suffered from longer equilibration times (~30 minutes,

316    more than double the 1.5 residence time) and therefore a slower response time, likely due to

317    increased surface effects of HCl after exiting the furnace. An optimal residence time of 1.5 seconds

318    was selected for all HCl-TCl experiments for its good conversion efficiency and reasonable

319    response time (see Table S3).



320
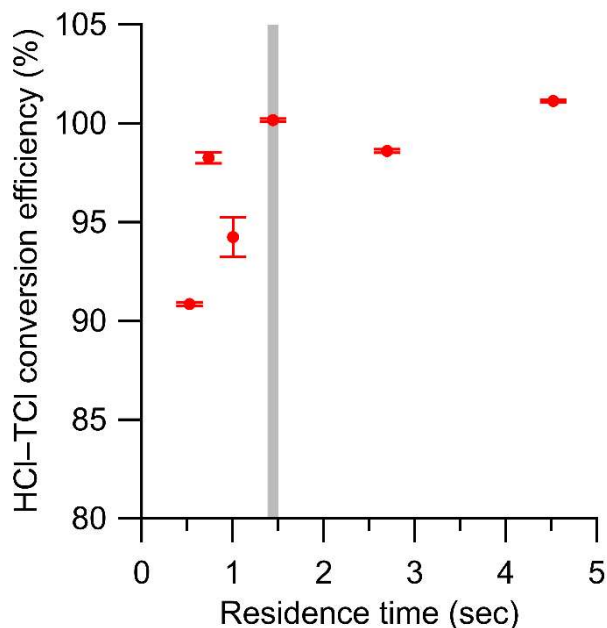
**Figure 2.** Conversion efficiency of DCM plotted against residence time in the HCl-TCl at 825 °C. Error bars represent the percent relative standard deviation of the measured HCl by the CRDS over ~30 minutes, after signal has plateaued. Grey vertical line denotes the selected residence time. Note that the error bars are represented by the precision of the instrument, and we expect there would be greater experiment-to-experiment variability.

326

327    **3.2. HCl-TCl conversion efficiency**

328    The efficiency of HCl throughput in the HCl-TCl was tested. Initial tests resulted in

329    transmission efficiencies of 81.2% ± 1.4 (n = 3) and 88.1% (n = 1) for 18 ppbv and 10 ppbv HCl,

330    respectively. At the inlet to the furnace, a small piece of the quartz tube is not heated. We

331    hypothesized that complete transmission of HCl was hindered through sorption to that portion of

332    quartz tube~~glass~~. Repeating the experiment with heat applied led to increased throughput

333    efficiencies of 85.7% (18 ppbv, n = 1) and 93.9% (10 ppbv, n = 1). Therefore, good HCl throughput

334    efficiency was demonstrated overall, with the cause of minor HCl losses identified to be sorption

335    losses to room temperature glass. Conversion of particulate chloride (pCl$^-$) was observed to take

16

336  place in the HCl-TCl (Figure S3), but once a filter was introduced the signal returned to

337  background levels-. Thus, to capture only gaseous TCl$_g$ from samples that may contain particulate

338  chloride, a particulate filter should be used.

339  The conversion efficiency of each of the ~~three~~ two ~~chosen organochlorines~~alkyl chloride and

340  one allyl chloride compounds using the HCl-TCl was tested at 5 different mixing ratios. ~~The~~

341  ~~mixing ratios tested for DCM were 41, 54, 80, 111, and 165 ppbv. The mixing ratios tested for CB~~

342  ~~were 3.5, 4.6, 6.8, 9.5, and 14 ppbv. The mixing ratios tested for DCP were 121, 259, 468, 651,~~

343  ~~and 967 ppbv.~~ See table S4 for summary of mixing ratios used, all lower mixing ratios were

344  generated by diluting the highest mixing ratio of each compound by chlorine-free zero air. All

345  three showed good linearity and near 1:1 correlation with the HCl expected to be formed from the

346  PD under standard operating conditions (Figure 3). Due to differences in PD emission rates, the

347  values in Figure 3 are normalized to the highest mixing ratio to visualize comparisons more easily.

348  ~~Under condition (1)~~ Wwith both Pt and propane the HCl-TCl conversion was 99.6 ± 3.2, 104.8 ±

349  5.6, and 102.7 ± 7.8% for DCM, CB, and DCP, respectively (Table 1), as the average conversion

350  efficiency ± relative standard deviation. From Figure 3 the comparison between expected and

351  measured TCl$_g$ is illustrated by near unity in the orthogonal distance regression slope (±1σ, the

352  error in the regression analysis), and was 0.996 ± 0.012, 1.048 ± 0.0~~06~~0, and 1.027 ± 0.061 for

353  DCM, CB, and DCP, respectively. With only the Pt catalyst ~~(condition (2))~~, the HCl-TCl

354  conversion was 80.7 ± 0.4, 54.1 ± 1.6, and 54.3 ± 3.5% for DCM, CB, and DCP, respectively

355  (Figure S~~3~~4, Table 1). This result indicates the added hydrogen source (propane) is needed to

356  promote R1. Although necessary in this laboratory scenario, some ambient conditions may be rich

357  enough hydrogen-containing molecules that excess propane is not needed. However, providing

358  propane in excess ensures the presence of an abundance of hydrogen atoms that can be readily

359 abstracted by Cl atoms via R1. When the Pt catalyst was removed (condition (3)), the HCl-TCl

360 conversion was 94.4 ± 4.6, 44.2 ± 0.9, and 41.7 ± 3.4% for DCM, CB, and DCP, respectively

361 (Figure S34, Table 1). The observed dependence of the Pt catalyst indicates that a reactive surface

362 is important to achieve complete thermolysis at 825 °C. The relatively higher conversion for DCM

363 in the absence of the Pt catalyst or hydrogen source may be attributed to its lower bond dissociation

364 energy (310 kJ mol$^{-1}$) compared to estimated bond dissociation energies for CB and DCP (CB



365

366
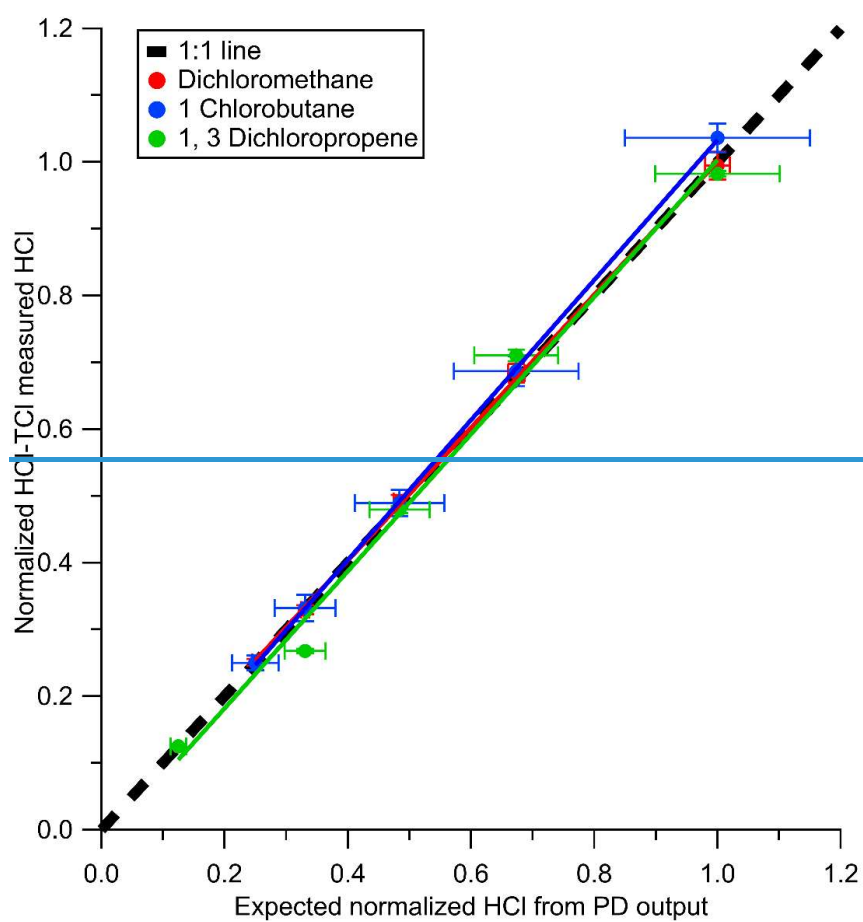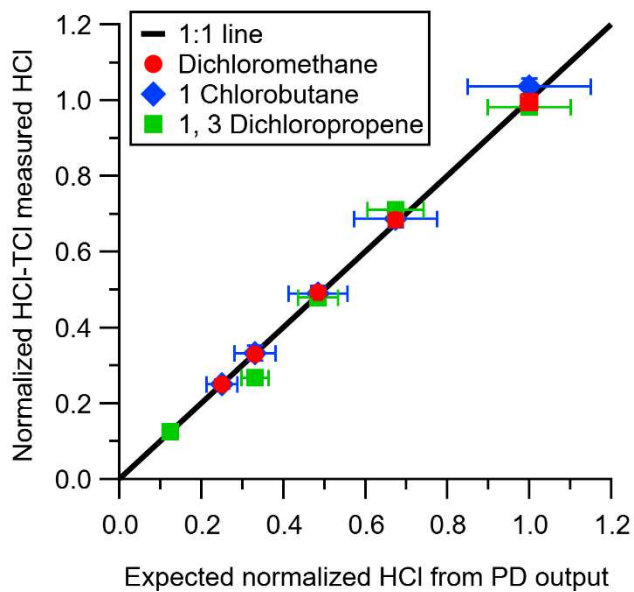
**Figure 3.** HCl measured by CRDS plotted against the expected HCl from HCl-TCl converted DCM (red circle), 1-chlorobutane (blue diamond), and 1,3-dichloropropene (green square) under condition (1). All values are normalized to the highest expected HCl concentration to better illustrate deviations from unity (dashed black line). Error bars on the y-axis represent $1\sigma$ in the HCl signal over 10 minutes. Error bars on the x-axis represent the uncertainty in the PD used to generate DCM.

373

19

374 **Table 1.** Conversion efficiency for tested Cl-containing~~organochlorine~~ compounds under
375 different~~the three~~ conditions (~~condition 1:~~ both Pt and propane; ~~condition 2:~~ Pt only; ~~condition 3:~~
376 propane only). Note that chlorobenzenes were only tested under final Pt and propane
377 conditions.~~Conversion efficiency was determined from the orthogonal distance regression slope~~
378 ~~and ± σ and propagated error from individual PDs.~~

| Tested TCl$_g$ species | Cl ~~B~~bond dissociation energy (kJ mol$^{-1}$) | Conversion efficiency (%) | | |
|---|---|---|---|---|
| | | ~~Condition 1~~Pt and propane | ~~Condition 2~~Pt only | ~~Condition 3~~Propane only |
| Dichloromethane (DCM)[a] | 310 | 99.6 ± 3.2 | 80.7 ± 2.4 | 94.4 ± 6.6 |
| 1-Chlorobutane (CB)[a] | 410 | 104.8 ± 5.6 | 54.1 ± 6.6 | 44.2 ± 5.9 |
| 1, 3-Dichloropropene (DCP)[a] | 350 | 102.7 ± 7.8 | 54.3 ± 5.2 | 41.7 ± 5.1 |
| Trichlorobenzene (TrCB)[b] | 400 | 97.0 ± 19.9 | | |
| Tetrachlorobenzene (TeCB)[b] | 400 | 90.6 ± 10.3 | | |
| Pentachlorobenzene (PeCB)[b] | 400 | 90.2 ± 14.8 | | |

379 [a]Conversion efficiency was determined from the orthogonal distance regression slope and ± σ and propagated error
380 from individual permeation devices.
381 [b]Conversion efficiency was determined directly by the quantity (mol) of HCl measured from liquid injections of 1
382 mM standards. The error represents ±σ of measurements for n = 5 (TrCB) or n = 4 (TeCB, PeCB) injections.
383

384 inferred from Table S2 (~410 kJ mol$^{-1}$), and DCP from tetrachloroethylene (350 kJ mol$^{-1}$ in Table

385 S1)). It is possible that a higher temperature could lead to full conversion of TCl$_g$ in the absence

386 of Pt catalyst; however, that was not explored in this study. To further validate the HCl-TCl, the

387 conversion efficiency of three aryl chlorine compounds were tested under the final operating

388 conditions (i.e., Condition 1, in the presence of both Pt and added propane). The TCl$_g$ measured

389 from the three aryl compounds was unity, within the uncertainty of the measurement (Table 1).

390 -       The results for all ~~three~~ six compounds show that the HCl-TCl is capable of complete

391 conversion of mono and polychlorinated species on sp$^3$ and sp$^2$ carbons using the determined

392 temperature and flow conditions. The complete thermolysis of the strongest C-Cl bond on the

393 primary alkyl chloride (CB) demonstrates the efficacy of the HCl-TCl. Breaking these relatively

394 strong C-Cl bonds, with consistent conversion efficiency across alkyl, allyl, and aryl C-Cl bonds,

395 is a good proof of concept for complete conversion of all bonds of similar or weaker bond energies

396 that characterize all other TCl$_g$. To practically validate the HCl-TCl under real-world conditions

397 with atmospherically relevant $TCl_g$ mixtures and mixing ratios we also deployed and configured

398 the system to measure outdoor and indoor air.

### 3.3. Performance metrics of HCl-TCl

400   Using a flow of zero air through the HCl-TCl, method limits of detection (LODs) were

401 calculated as three times the Allan-Werle deviation (Figure 4) when overflowing a 20 cm inlet

402 (3.17 mm i.d.) with zero air for one hour. The LODs determined in the CRDS measurements for 2

403 second, 1 minute, 5 minute, and 1 hour integration times were 73, 15, 10, and 8 pptv, respectively.

404 The response time of the instrument was assessed during experiments with DCM, CB, and CP.

405 The time for the signal to decay after removal of the PDs was determined to 37 % (1/e) and 90 %

406 ($t_{90}$) of the maximum signal. The maximum time to achieve 1/e was 23 seconds, while the

407 maximum time to achieve $t_{90}$ was 189 seconds (Table S3). These are comparable to the response

408 times for the HCl CRDS instrument itself (Furlani et al. 2021), suggesting the addition of the inlet

409 furnace has a modest impact on the residence time. Given the high mixing ratios used to test the

410 response times, we argue that under most conditions relevant to indoor and outdoor atmospheric

411 chemistry, a sample integration time of one minute will minimize any time response effects. Data

412 for outdoor and indoor sampling described in Sections 3.4 and 3.5 were therefore averaged to one

413 minute. During all experiments with gaseous reagents, no evidence of catalyst performance

414 degradation was observed.
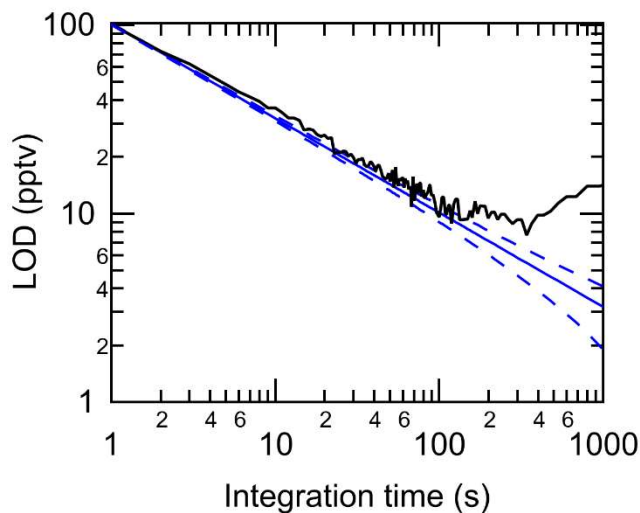
**Figure 4.** Allan-Werle deviation (3σ) in the HCl-TCl purged with zero-air (black line) shown with the ideal deviation (no drift, solid blue line) and associated error in the deviation (dashed blue line).

### 3.3.3.4. HCl-TCl applications to outdoor air

We deployed the system to measure ambient outdoor air, which we compare to the expected

TCl$_g$ range from complete thermolysis of ~~total Cl~~previously measured Cl-containing compounds,

expected to be between 3.3 and 19 ppbv (Table S1). Global background levels of long-lived

chlorine-containing species (LLCl$_g$) are well established (WMO (World Meteorological

Organization), 2018) and were calculated by equation 3~~2~~ using data from Table S1:

LLCl$_g$ = 3*[CCl$_3$F] + 2*[CCl$_2$F$_2$] + 4*[CCl$_2$FCCl$_2$F] + 4*[CCl$_3$CClF$_2$] + 3*[CCl$_3$CF$_3$] +
2*[CClF$_2$CClF$_2$] + 2*[CCl$_2$FCF$_3$] + [CClF$_2$CF$_3$] + [CHClF$_2$] + [CH$_2$ClCF$_3$] + 2*[CH$_3$CCl$_2$F] +
[CBrClF$_2$] + 4*[CCl$_4$]            E3

A global background for LLCl$_g$ of approximately 2.6 ppbv is expected ~~if only considering the~~

~~controlled very long-lived species~~ ((WMO (World Meteorological Organization), 2018), Table

S1). ~~The effects of particulate chloride on TCl$_g$ conversion were not explored here. The conditions~~

~~required to convert chloride to chlorine atoms is typically achieved using high energy photons or~~

~~by electron beams, which deliver energy much greater than possible in our system (Delahay, 1982;~~

~~Kurepa and Belic, 1978). Thus, chloride, if it enters the system, is assumed to not be converted~~

~~and measured. The apparatus subsampled off a main inlet pulling ambient air (Figure 4) in summer~~ ~~(August 6) and winter (November 17–19).~~ The maximum, minimum, and ~~mean~~ median of observed ambient TCl$_g$ ~~on August 6~~ w~~er~~eas ~~6.05~~36.3, ~~3.4~~2.0, and ~~4.2~~3.1 ppbv, respectively~~, and~~ ~~was 3.5, 2.0, and 2.5 ppbv respectively from November 17–19~~ (Figure 5). Measurements of HCl alone were not made during these periods but reported ranges of HCl mixing ratios for this sampling location from Furlani et al. (2021) and Angelucci et al. (2021) ~~are~~ were typically below 110 pptv, with intermittent events up to 600 pptv. As expected, most ambient TCl$_g$ measurements were above the expected mixing ratio of LLCl$_g$. There is clear evidence of TCl$_g$ sources beyond LLCl$_g$ at the sampling site, with several plumes of elevated TCl$_g$ intercepted. For example, the maximum TCl$_g$ measurement was made in a plume just after noon on July 7. Another plume was detected on July 11, with a maximum TCl$_g$ of 42.1 ppbv. Though the purpose of this study was not to determine sources of TCl$_g$, we observed that plumes containing elevated TCl$_g$ arrived from the S-SW of the sampling site, where several facilities that had reported tens to thousands of kg of yearly emissions to air of Cl-containing species are located (Figure S5). ~~Mixing ratios of TCl$_g$~~ ~~were higher in the summer season when compared to the winter, suggesting a seasonal variance~~ ~~on the levels of TCl$_g$. The mean August TCl$_g$ was 60% higher than the expected baseline of known~~ ~~long lived species. In contrast, levels of TCl$_g$ in the during the winter were near the expected global~~ ~~baseline. We generally observed higher TCl$_g$ during periods of lower relative humidity (RH),~~ ~~illustrated by the lower levels of TCl$_g$ and high RH observed during November. There was no~~ ~~observed impact on observed TCl$_g$ due to changes in wind direction or wind speed and likely~~ ~~indicates TCl$_g$ is relatively well mixed. Our observed seasonal differences in TCl$_g$ could have been~~ ~~caused, in part, by differences in meteorology (i.e., higher temperature in summer, higher relative~~ ~~humidity in winter) through changes in mixing and/or deposition. However, it seems likely that~~

457    ~~higher summer emissions, which have been observed for individual chlorinated species (Bin et al.,~~

458    ~~2014; Melymuk et al., 2012; Zhang et al., 2014) played an important role in the higher summertime~~

459    ~~TCl_g. Rapid temporal changes in TCl_g indicate the utility of an in-situ technique, which could be~~

460    ~~used to constrain sources and sinks of TCl_g.~~



461
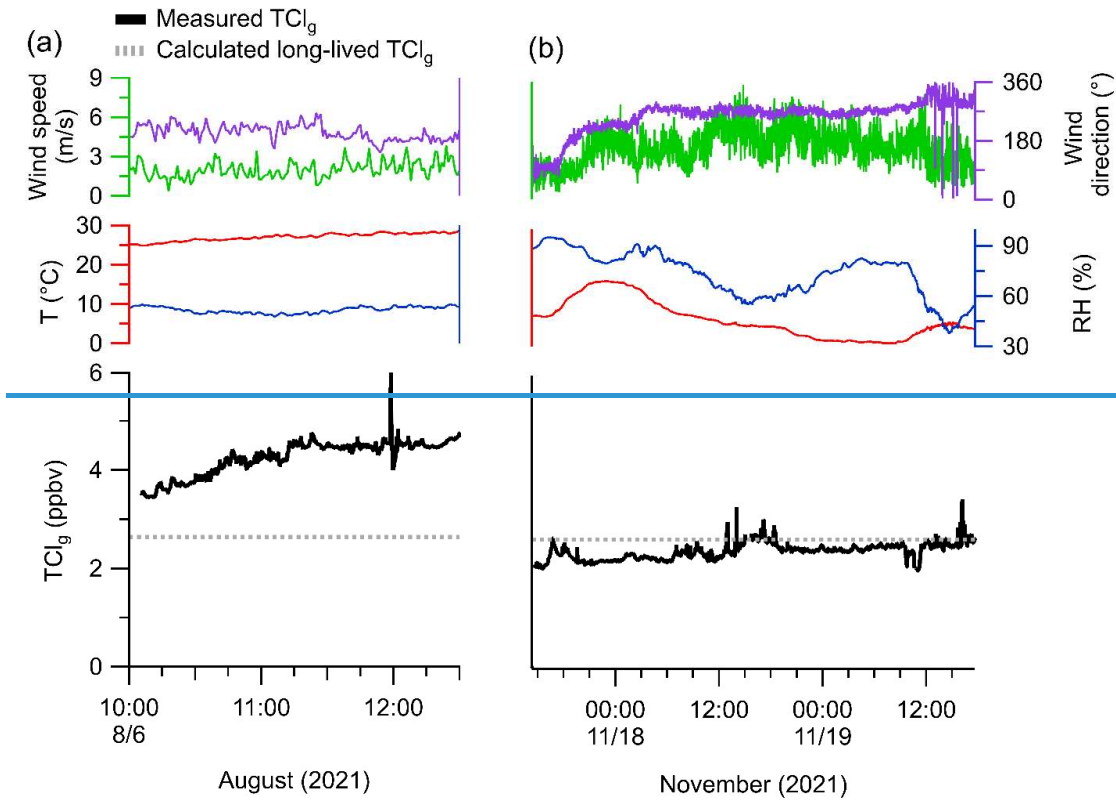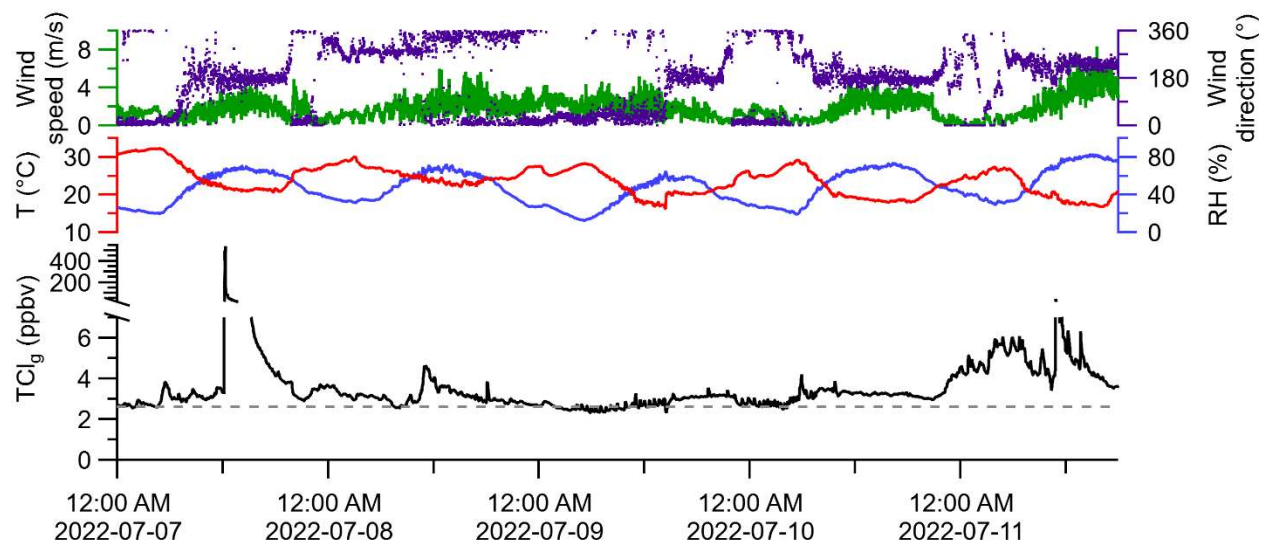
**Figure 45.** Monitoring meteorological conditions and ~~one-minute averaged~~ TCl$_g$ in outdoor air through HCl-TCl~~; (a)~~ from ~~10 AM to 1 PM August 6, and (b) from 12 PM November~~ July 7 to 11, 2022~~17 to 6 PM November 19~~. Grey dashed line represents the background mixing ratio for ~~LLCl~~long-lived TCl$_g$ species from Table S1.

### 3.4.3.5.    HCl-TCl application to indoor cleaning

We applied a chlorine-based cleaning product four times in a well-lit indoor room and measured TCl$_g$ using the HCl-TCl and HOCl analyzer during three of the cleaning events (Figure 65). One cleaning experiment was done without the HCl-TCl and had a maximum of 370 pptv HCl. These levels are comparable to peak HCl levels of ~500 pptv observed from surface application of bleach (Dawe et al., 2019). Consistent with previous speciated measurements (Mattila et al., 2020; Wong et al., 2017), HCl, HOCl, and TCl$_g$ levels increased rapidly over ~5 minutes after the application of the cleaning product. The maximum levels of TCl$_g$ from HCl-TCl during application 1, 2, and 3, were 49.2, 80.0, and 69.7 ppbv, respectively. The maximum levels of HOCl from applications 1, 2, and 3, were 19.6, 24.2, and 16.8 ppbv, respectively, corresponding to 24 to 40 % of peak TCl$_g$ and 14 to 22 % of integrated TCl$_g$. These TCl$_g$ levels were several times higher than observed in outdoor air (Section 3.3) and were within the range expected from previous experiments (Table S1). The levels of chlorinated species observed during bleaching events is

25

480    variable, between 15 to 100s of ppbv (Mattila et al., 2020; Odabasi, 2008; Wang et al., 2019; Wong

481    et al., 2017). By comparison, our highest observed mixing ratio was 80 ppbv. Because the

482    multiphase chemical processes involved in bleach application are complex and poorly understood,

483    it is difficult to compare levels between similar studies, given that the underlying ambient

484    conditions can be very different. In addition, physical parameters, such as volume of cleaning

485    solution applied, room size, and ventilation, can all affect observed mixing ratios. For example,

486    studies have observed that gaseous $NH_3$ partitioning into aqueous bleach can produce large and

487    variable amounts of chloramines, $NH_2Cl$, $NHCl_2$, and $NCl_3$ (Mattila et al., 2020; Wong et al.,

488    2017). In our experiments, there was on average $82 \pm 4$ % of integrated $TCl_g$ that could not be

489    accounted for by the HOCl measurement.for which we cannot account. Additional chlorinated

490    species have previously been observed to be emitted from surface bleaching include $ClNO_2$,

491    $NH_2Cl$, $NHCl_2$, $NCl_3$, and several chlorinated organics (Odabasi, 2008; Mattila et al., 2020; Wong

492    et al., 2017) which likely also contributed to our measured $TCl_g$. We observed that $TCl_g$ decayed

493    ~15% faster than the air exchange rate ($0.72\ h^{-1}$), indicating additional chemical loss pathways or

494    surface interactions (Figure S46). We observed a shorter lifetime of HOCl relative to $TCl_g$, which

495    is consistent with faster decay rates observed for HOCl and similar $TCl_g$ species by Wong et. al.,

496    (2017). The HOCl started decreasing after ~300 s had elapsed while the $TCl_g$ levels were still

497    increasing. This suggests that reactions involving HOCl may have led to additional $TCl_g$ species,

498    which has been observed in laboratory studies (Wang et al., 2019).

499        In-situ measurements of $TCl_g$ could provide additional insight into sources of chlorinated

500    species to indoor environments by creating a total inventory from which the contributions of

501    individual measured species can be compared and used to elucidate unknown $TCl_g$ levels and

502    mechanisms in real-time. Furthermore, several chlorinated species that have previously been

503     observed to be emitted from surface bleaching, including $Cl_2$, $HOCl$, $ClNO_2$, $NH_2Cl$, $NHCl_2$, and

504     $NCl_3$ (Mattila et al., 2020; Wong et al., 2017), have been measured by chemical ionization mass

505     spectrometry (CIMS). Quantifying chlorinated species using CIMS remains challenging due to the

506     required calibrations and difficulty in generating pure gas phase standards. It is therefore desirable

507     to have a technique such as the one proposed in this study that does not require calibrations or

508     knowledge of potential unknown $TCl_g$ species. A combination of the two methods would help

509     constrain the total levels while still observing speciation for key $TCl_g$ species.



510
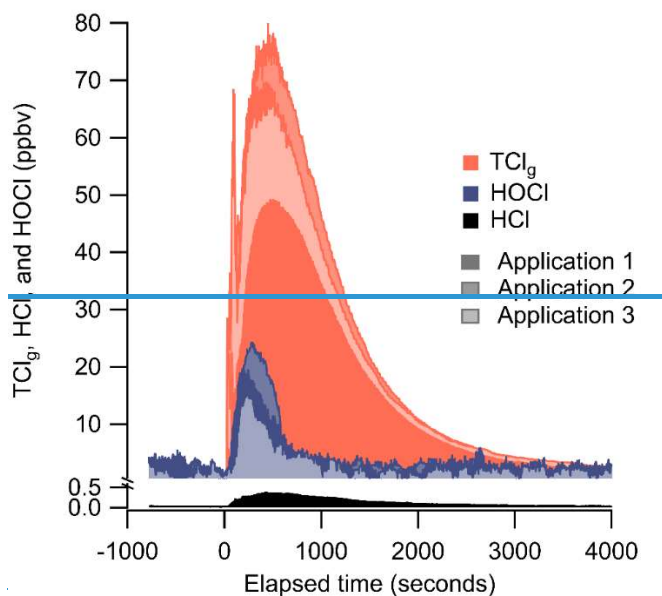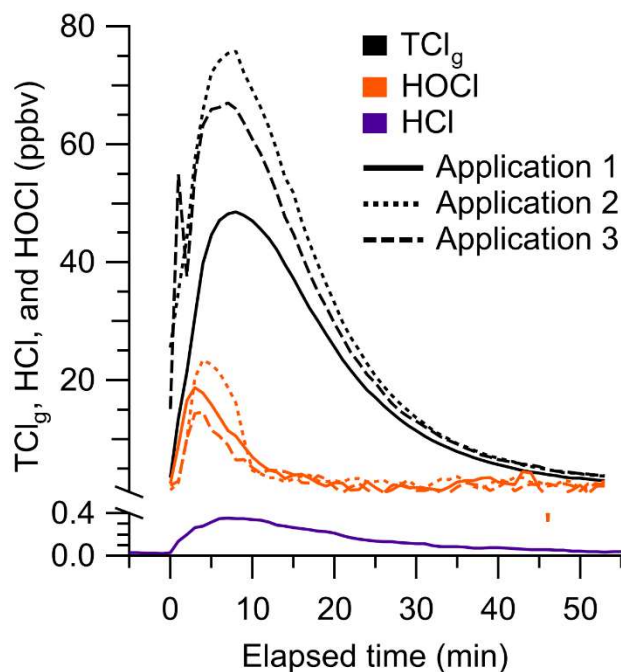
**Figure** ~~5~~6. <u>One-minute average </u>HCl (<u>purple</u>~~black~~), HOCl (<u>orange</u>~~dark blue~~), and TCl$_g$ (<u>black</u>~~orange~~) observed during cleaning spray events. Mixing ratios were background corrected prior to each cleaning event. Each subsequent application of cleaner is illustrated by a lighter shade for HOCl and TCl$_g$.

## 4. Conclusions

In this work we developed, optimized, validated, and applied a method capable of converting TCl$_g$ into gaseous HCl ~~amenable~~ for <u>detection by </u>CRDS ~~detection~~. Our TCl$_g$ measurement technique, the HCl-TCl, is composed of a platinum catalyst mesh inside a quartz glass flow tube all contained within a split-tube furnace. The temperature and flow rate were optimized at 825 °C and 1.5 seconds, respectively using DCM. These conditions were validated by the complete conversion of organochlorine compounds with strong C-Cl bonds. The HCl-TCl was used to measure TCl$_g$ outdoors, observing a range of 2.0~~–~~<u> to 536.3</u>~~6.0~~ ppbv. Levels <u>mostly </u>~~were~~ ~~comparable to (winter) or~~ exceeded ~~(summer) ~~the ~~calculated ~~<u>expected </u>background mixing ratio of ~~long-lived T~~<u>LL</u>Cl$_g$. We also applied the HCl-TCl to an indoor environment during commercial bleach spray cleaning events and observed varying increases in TCl$_g$ (50–80 ppbv), which was in

28

528    reasonable agreement with levels observed in previous speciated measurements. The agreement of

529    HCl-TCl outdoor and indoor measurements with available bottom-up estimates indicates its

530    efficacy under real-world scenarios. Rapid changes in $TCl_g$ were observed in both outdoor and

531    indoor environments indicating the utility of an in-situ technique to constrain the sources and

532    chemistry of $TCl_g$, as well as its impact on air quality, climate, and health. We anticipate this

533    approach could be used in several applications, including comparisons to speciated measurements

534    of chlorinated compounds and to further explore Cl reactivity and cycling with respect for indoor

535    and outdoor $TCl_g$.

## Acknowledgements

## Author contributions

545    TCF, RY, JS, and LRC collected and analyzed the data. TCF, RY, LRC, and CJY conceived of

546    and designed the experiments with input from PME and TFK. Funding was obtained by TFK and

547    CJY. The manuscript was written by TCF, RY, and CJY with input from all authors.

## Data availability

549 Outdoor and indoor datasets submitted to Federated Research Data Repository as Furlani, T.C.,

550 Ye, R., Stewart, J., Crilley, L.R., Edwards, P.M., Kahan,T.F., Young, C.J. (2022). Outdoor and

551 indoor gaseous total chlorine measurement in Toronto Canada. Federated Research Data

552 Repository. DOI will be updated when available.

553 **Competing interests**

554 The authors declare no competing interests.

555 **5. References**

556 Adcock, K. E., Reeves, C. E., Gooch, L. J., Leedham Elvidge, E. C., Ashfold, M. J.,
557 Brenninkmeijer, C. A. M., Chou, C., Fraser, P. J., Langenfelds, R. L., Mohd Hanif, N.,
558 O'Doherty, S., Oram, D. E., Ou-Yang, C.-F., Phang, S. M., Samah, A. A., Röckmann, T.,
559 Sturges, W. T., and Laube, J. C.: Continued increase of CFC-113a ($CCl_3CF_3$) mixing ratios in
560 the global atmosphere: emissions, occurrence and potential sources, Atmos. Chem. Phys., 18,
561 4737–4751, https://doi.org/10.5194/acp-18-4737-2018, 2018.

562 Andrews, S. J., Carpenter, L. J., Apel, E. C., Atlas, E., Donets, V., Hopkins, J. R., Hornbrook, R.
563 S., Lewis, A. C., Lidster, R. T., Lueb, R., Minaeian, J., Navarro, M., Punjabi, S., Riemer, D., and
564 Schauffler, S.: A comparison of very short lived halocarbon (VSLS) and DMS aircraft
565 measurements in the tropical west Pacific from CAST, ATTREX and CONTRAST, Atmos.
566 Meas. Tech., 9, 5213–5225, https://doi.org/10.5194/amt-9-5213-2016, 2016.

567 Berg, W. W., Crutzen, P. J., Grahek, F. E., Gitlin, S. N., and Sedlacek, W. A.: First
568 measurements of total chlorine and bromine in the lower stratosphere, Geophys Res Lett, 7, 937–
569 940, https://doi.org/https://doi.org/10.1029/GL007i011p00937, 1980.

570 Blankenship, A., Chang, D. P. Y., Jones, A. D., Kelly, P. B., Kennedy, I. M., Matsumura, F.,
571 Pasek, R., and Yang, G.: Toxic combustion by-products from the incineration of chlorinated
572 hydrocarbons and plastics, Chemosphere, 28, 183–196,
573 https://doi.org/https://doi.org/10.1016/0045-6535(94)90212-7, 1994.

574 Butz, A., Dinger, A. S., Bobrowski, N., Kostinek, J., Fieber, L., Fischerkeller, C., Giuffrida, G.
575 B., Hase, F., Klappenbach, F., Kuhn, J., Lübcke, P., Tirpitz, L., and Tu, Q.: Remote sensing of
576 volcanic $CO_2$, HF, HCl, $SO_2$, and BrO in the downwind plume of Mt. Etna, Atmos Meas Tech,
577 10, 1–14, https://doi.org/10.5194/amt-10-1-2017, 2017.

578 Dawe, K. E. R., Furlani, T. C., Kowal, S. F., Kahan, T. F., Vandenboer, T. C., and Young, C. J.:
579 Formation and emission of hydrogen chloride in indoor air, Indoor Air, 70–78,
580 https://doi.org/10.1111/ina.12509, 2019.

581    Doucette, W. J., Wetzel, T. A., Dettenmaier, E., and Gorder, K.: Emission rates of chlorinated
582    volatile organics from new and used consumer products found during vapor intrusion
583    investigations: Impact on indoor air concentrations, Environ Forensics, 19, 185–190,
584    https://doi.org/10.1080/15275922.2018.1475433, 2018.

585    Fernando, S., Jobst, K. J., Taguchi, V. Y., Helm, P. A., Reiner, E. J., and McCarry, B. E.:
586    Identification of the Halogenated Compounds Resulting from the 1997 Plastimet Inc. Fire in
587    Hamilton, Ontario, using Comprehensive Two-Dimensional Gas Chromatography and
588    (Ultra)High Resolution Mass Spectrometry, Environ Sci Technol, 48, 10656–10663,
589    https://doi.org/10.1021/es503428j, 2014.

590    Finlayson-Pitts, B. J.: Chlorine Atoms as a Potential Tropospheric Oxidant in the Marine
591    Boundary Layer, Research on Chemical Intermediates, 19, 235–249,
592    https://doi.org/10.1163/156856793X00091, 1993.

593    Furlani, T. C., Veres, P. R., Dawe, K. E. R., Neuman, J. A., Brown, S. S., VandenBoer, T. C.,
594    and Young, C. J.: Validation of a new cavity ring-down spectrometer for measuring tropospheric
595    gaseous hydrogen chloride, Atmos. Meas. Tech. Discuss., 2021, 1–30,
596    https://doi.org/10.5194/amt-2021-105, 2021.

597    Giardino, N. J. and Andelman, J. B.: Characterization of the emissions of trichloroethylene,
598    chloroform, and  1,2-dibromo-3-chloropropane in a full-size, experimental shower., J Expo Anal
599    Environ Epidemiol, 6, 413–423, 1996.

600    Hardy, J. E. and Knarr, J. J.: Technique for Measuring the Total Concentration of Gaseous Fixed
601    Nitrogen Species, J Air Pollut Control Assoc, 32, 376–379,
602    https://doi.org/10.1080/00022470.1982.10465412, 1982.

603    Haskins, J. D., Jaeglé, L., Shah, V., Lee, B. H., Lopez-Hilfiker, F. D., Campuzano-Jost, P.,
604    Schroder, J. C., Day, D. A., Guo, H., Sullivan, A. P., Weber, R., Dibb, J., Campos, T., Jimenez,
605    J. L., Brown, S. S., and Thornton, J. A.: Wintertime Gas-Particle Partitioning and Speciation of
606    Inorganic Chlorine in the Lower Troposphere Over the Northeast United States and Coastal
607    Ocean, Journal of Geophysical Research: Atmospheres, 123, 12,812-897,916,
608    https://doi.org/10.1029/2018JD028786, 2018.

609    Henschler, D.: Toxicity of Chlorinated Organic Compounds: Effects of the Introduction of
610    Chlorine in Organic Molecules, Angewandte Chemie International Edition in English, 33, 1920–
611    1935, https://doi.org/https://doi.org/10.1002/anie.199419201, 1994.

612    Kannan, K., Kawano, M., Kashima, Y., Matsui, M., and Giesy, J. P.: Extractable
613    Organohalogens (EOX) in Sediment and Biota Collected at an Estuarine Marsh near a Former
614    Chloralkali Facility, Environ Sci Technol, 33, 1004–1008, https://doi.org/10.1021/es9811142,
615    1999.

616    Kato, M., Urano, K., and Tasaki, T.: Development of Semi- and Nonvolatile Organic Halogen as
617    a New Hazardous Index of Flue Gas, Environ Sci Technol, 34, 4071–4075,
618    https://doi.org/10.1021/es000881+, 2000.

619 Kawano, M., Falandysz, J., and Wakimoto, T.: Instrumental neutron activation analysis of
620 extractable organohalogens in the Antarctic Weddell seal ( Leptonychotes weddelli ), J
621 Radioanal Nucl Chem, 272, 501–504, https://doi.org/10.1007/s10967-007-0611-5, 2007.

622 Keene, William. C., Khalil, M. A. K., Erickson, David. J., McCulloch, A., Graedel, T. E., Lobert,
623 J. M., Aucott, M. L., Gong, S. L., Harper, D. B., Kleiman, G., Midgley, P., Moore, R. M.,
624 Seuzaret, C., Sturges, W. T., Benkovitz, C. M., Koropalov, V., Barrie, L. A., and Li, Y. F.:
625 Composite global emissions of reactive chlorine from anthropogenic and natural sources:
626 Reactive Chlorine Emissions Inventory, Journal of Geophysical Research: Atmospheres, 104,
627 8429–8440, https://doi.org/10.1029/1998JD100084, 1999.

628 Khalil, M. A. K., Moore, R. M., Harper, D. B., Lobert, J. M., Erickson, D. J., Koropalov, V.,
629 Sturges, W. T., and Keene, W. C.: Natural emissions of chlorine-containing gases: Reactive
630 Chlorine Emissions Inventory, Journal of Geophysical Research: Atmospheres, 104, 8333–8346,
631 https://doi.org/10.1029/1998JD100079, 1999.

632 Lao, M., Crilley, L. R., Salehpoor, L., Furlani, T. C., Bourgeois, I., Neuman, J. A., Rollins, A.
633 W., Veres, P. R., Washenfelder, R. A., Womack, C. C., Young, C. J., and VandenBoer, T. C.: A
634 portable, robust, stable and tunable calibration source for gas-phase nitrous acid (HONO), Atmos
635 Meas Tech, 13, 5873–5890, https://doi.org/10.5194/amt-13-5873-2020, 2020.

636 Lobert, J. M., Keene, W. C., Logan, J. A., and Yevich, R.: Global chlorine emissions from
637 biomass burning: Reactive Chlorine Emissions Inventory, Journal of Geophysical Research
638 Atmospheres, 104, 8373–8389, https://doi.org/10.1029/1998JD100077, 1999.

639 Maris, C., Chung, M. Y., Lueb, R., Krischke, U., Meller, R., Fox, M. J., and Paulson, S. E.:
640 Development of instrumentation for simultaneous analysis of total non-methane organic carbon
641 and volatile organic compounds in ambient air, Atmos Environ, 37, 149–158,
642 https://doi.org/https://doi.org/10.1016/S1352-2310(03)00387-X, 2003.

643 Massin, N., Bohadana, A. B., Wild, P., Héry, M., Toamain, J. P., and Hubert, G.: Respiratory
644 symptoms and bronchial responsiveness in lifeguards exposed to nitrogen trichloride in indoor
645 swimming pools., Occup Environ Med, 55, 258 LP – 263, https://doi.org/10.1136/oem.55.4.258,
646 1998.

647 Mattila, J. M., Lakey, P. S. J., Shiraiwa, M., Wang, C., Abbatt, J. P. D., Arata, C., Goldstein, A.
648 H., Ampollini, L., Katz, E. F., DeCarlo, P. F., Zhou, S., Kahan, T. F., Cardoso-Saldaña, F. J.,
649 Ruiz, L. H., Abeleira, A., Boedicker, E. K., Vance, M. E., and Farmer, D. K.: Multiphase
650 Chemistry Controls Inorganic Chlorinated and Nitrogenated Compounds in Indoor Air during
651 Bleach Cleaning, Environ Sci Technol, 54, 1730–1739, https://doi.org/10.1021/acs.est.9b05767,
652 2020.

653 Miyake, Y., Kato, M., and Urano, K.: A method for measuring semi- and non-volatile organic
654 halogens by combustion ion chromatography, J Chromatogr A, 1139, 63–69,
655 https://doi.org/https://doi.org/10.1016/j.chroma.2006.10.078, 2007a.

Miyake, Y., Yamashita, N., Rostkowski, P., So, M. K., Taniyasu, S., Lam, P. K. S., and Kannan, K.: Determination of trace levels of total fluorine in water using combustion ion chromatography for fluorine: A mass balance approach to determine individual perfluorinated chemicals in water, J Chromatogr A, 1143, 98–104, https://doi.org/https://doi.org/10.1016/j.chroma.2006.12.071, 2007b.

Miyake, Y., Yamashita, N., So, M. K., Rostkowski, P., Taniyasu, S., Lam, P. K. S., and Kannan, K.: Trace analysis of total fluorine in human blood using combustion ion chromatography for fluorine: A mass balance approach for the determination of known and unknown organofluorine compounds, J Chromatogr A, 1154, 214–221, https://doi.org/https://doi.org/10.1016/j.chroma.2007.03.084, 2007c.

Montzka, S. A., Dutton, G. S., Portmann, R. W., Chipperfield, M. P., Davis, S., Feng, W., Manning, A. J., Ray, E., Rigby, M., Hall, B. D., Siso, C., Nance, J. D., Krummel, P. B., Mühle, J., Young, D., O'Doherty, S., Salameh, P. K., Harth, C. M., Prinn, R. G., Weiss, R. F., Elkins, J. W., Walter-Terrinoni, H., and Theodoridi, C.: A decline in global CFC-11 emissions during 2018−2019, Nature, 590, 428–432, https://doi.org/10.1038/s41586-021-03260-5, 2021.

Nuckols, J. R., Ashley, D. L., Lyu, C., Gordon, S. M., Hinckley, A. F., and Singer, P.: Influence of tap water quality and household water use activities on indoor air and internal dose levels of trihalomethanes, Environ Health Perspect, 113, 863–870, https://doi.org/10.1289/ehp.7141, 2005.

Odabasi, M.: Halogenated Volatile Organic Compounds from the Use of Chlorine-Bleach-Containing Household Products, Environ Sci Technol, 42, 1445–1451, https://doi.org/10.1021/es702355u, 2008.

Odabasi, M., Elbir, T., Dumanoglu, Y., and Sofuoglu, S.: Halogenated volatile organic compounds in chlorine-bleach-containing household products and implications for their use, Atmos Environ, 92, 376–383, https://doi.org/10.1016/j.atmosenv.2014.04.049, 2014.

Pan, L. L., Atlas, E. L., Salawitch, R. J., Honomichl, S. B., Bresch, J. F., Randel, W. J., Apel, E. C., Hornbrook, R. S., Weinheimer, A. J., Anderson, D. C., Andrews, S. J., Baidar, S., Beaton, S. P., Campos, T. L., Carpenter, L. J., Chen, D., Dix, B., Donets, V., Hall, S. R., Hanisco, T. F., Homeyer, C. R., Huey, L. G., Jensen, J. B., Kaser, L., Kinnison, D. E., Koenig, T. K., Lamarque, J.-F., Liu, C., Luo, J., Luo, Z. J., Montzka, D. D., Nicely, J. M., Pierce, R. B., Riemer, D. D., Robinson, T., Romashkin, P., Saiz-Lopez, A., Schauffler, S., Shieh, O., Stell, M. H., Ullmann, K., Vaughan, G., Volkamer, R., and Wolfe, G.: The Convective Transport of Active Species in the Tropics (CONTRAST) Experiment, Bull Am Meteorol Soc, 98, 106–128, https://doi.org/10.1175/BAMS-D-14-00272.1, 2017.

Prinn, R. G., Weiss, R. F., Arduini, J., Arnold, T., DeWitt, H. L., Fraser, P. J., Ganesan, A. L., Gasore, J., Harth, C. M., Hermansen, O., Kim, J., Krummel, P. B., Li, S., Loh, Z. M., Lunder, C. R., Maione, M., Manning, A. J., Miller, B. R., Mitrevski, B., Mühle, J., O'Doherty, S., Park, S., Reimann, S., Rigby, M., Saito, T., Salameh, P. K., Schmidt, R., Simmonds, P. G., Steele, L. P., Vollmer, M. K., Wang, R. H., Yao, B., Yokouchi, Y., Young, D., and Zhou, L.: History of

chemically and radiatively important atmospheric gases from the Advanced Global Atmospheric Gases Experiment (AGAGE), Earth Syst. Sci. Data, 10, 985–1018, https://doi.org/10.5194/essd-10-985-2018, 2018.

Raff, J. D., Njegic, B., Chang, W. L., Gordon, M. S., Dabdub, D., Gerber, R. B., and Finlayson-Pitts, B. J.: Chlorine activation indoors and outdoors via surface-mediated reactions of nitrogen oxides with hydrogen chloride, Proceedings of the National Academy of Sciences, 106, 13647 LP – 13654, https://doi.org/10.1073/pnas.0904195106, 2009.

Riedel, T. P., Wolfe, G. M., Danas, K. T., Gilman, J. B., Kuster, W. C., Bon, D. M., Vlasenko, A., Li, S.-M., Williams, E. J., Lerner, B. M., Veres, P. R., Roberts, J. M., Holloway, J. S., Lefer, B., Brown, S. S., and Thornton, J. A.: An MCM modeling study of nitryl chloride ($ClNO_2$) impacts on oxidation, ozone production and nitrogen oxide partitioning in polluted continental outflow, Atmos. Chem. Phys., 14, 3789–3800, https://doi.org/10.5194/acp-14-3789-2014, 2014.

Roberts, J. M., Bertman, S. B., Jobson, T., Niki, H., and Tanner, R.: Measurement of total nonmethane organic carbon (Cy): Development and application at Chebogue Point, Nova Scotia, during the 1993 North Atlantic Regional Experiment campaign, Journal of Geophysical Research: Atmospheres, 103, 13581–13592, https://doi.org/https://doi.org/10.1029/97JD02240, 1998.

Saiz-Lopez, A. and Von Glasow, R.: Reactive halogen chemistry in the troposphere, Chem Soc Rev, 41, 6448–6472, https://doi.org/10.1039/c2cs35208g, 2012.

Schwartz-Narbonne, H., Wang, C., Zhou, S., Abbatt, J. P. D., and Faust, J.: Heterogeneous Chlorination of Squalene and Oleic Acid, Environ Sci Technol, 53, 1217–1224, https://doi.org/10.1021/acs.est.8b04248, 2019.

Shepherd, J. L., Corsi, R. L., and Kemp, J.: Chloroform in Indoor Air and Wastewater: The Role of Residential Washing Machines., J Air Waste Manag Assoc, 46, 631–642, https://doi.org/10.1080/10473289.1996.10467497, 1996.

Sherwen, T., Schmidt, J. A., Evans, M. J., Carpenter, L. J., Großmann, K., Eastham, S. D., Jacob, D. J., Dix, B., Koenig, T. K., Sinreich, R., Ortega, I., Volkamer, R., Saiz-Lopez, A., Prados-Roman, C., Mahajan, A. S., and Ordóñez, C.: Global impacts of tropospheric halogens (Cl, Br, I) on oxidants and composition in GEOS-Chem, Atmos. Chem. Phys., 16, 12239–12271, https://doi.org/10.5194/acp-16-12239-2016, 2016.

Simpson, W. R., Brown, S. S., Saiz-Lopez, A., Thornton, J. A., and Von Glasow, R.: Tropospheric Halogen Chemistry: Sources, Cycling, and Impacts, Chem Rev, 115, 4035–4062, https://doi.org/10.1021/cr5006638, 2015.

Solomon, S.: Stratospheric ozone depletion: A review of concepts and history, Reviews of Geophysics, 37, 275–316, https://doi.org/10.1029/1999RG900008, 1999.

Stockwell, C. E., Kupc, A., Witkowski, B., Talukdar, R. K., Liu, Y., Selimovic, V., Zarzana, K. J., Sekimoto, K., Warneke, C., Washenfelder, R. A., Yokelson, R. J., Middlebrook, A. M., and Roberts, J. M.: Characterization of a catalyst-based conversion technique to measure total

733  particulate nitrogen and organic carbon and comparison to a particle mass measurement
734  instrument, Atmos. Meas. Tech., 11, 2749–2768, https://doi.org/10.5194/amt-11-2749-2018,
735  2018.

736  Stubbs, A., Lao, M., Wang, C., Abbatt, J., Hoffnagle, J., VandenBoer, T., and Kahan, T.: Near-
737  source hypochlorous acid emissions from indoor bleach cleaning, Environ Sci Process Impacts,
738  Submitted, 2022.

739  Unsal, V., Cicek, M., and Sabancilar, İ.: Toxicity of carbon tetrachloride, free radicals and role
740  of antioxidants, Rev Environ Health, 36, 279–295, https://doi.org/doi:10.1515/reveh-2020-0048,
741  2021.

742  Veres, P., Gilman, J. B., Roberts, J. M., Kuster, W. C., Warneke, C., Burling, I. R., and de
743  Gouw, J.: Development and validation of a portable gas phase standard  generation and
744  calibration system for volatile organic compounds, Atmos. Meas. Tech., 3, 683–691,
745  https://doi.org/10.5194/amt-3-683-2010, 2010.

746  Wang, C., Collins, D. B., and Abbatt, J. P. D.: Indoor Illumination of Terpenes and Bleach
747  Emissions Leads to Particle Formation and Growth, Environ Sci Technol, 53, 11792–11800,
748  https://doi.org/10.1021/acs.est.9b04261, 2019.

749  White, C. W. and Martin, J. G.: Chlorine Gas Inhalation, Proc Am Thorac Soc, 7, 257–263,
750  https://doi.org/10.1513/pats.201001-008SM, 2010.

751  WMO (World Meteorological Organization): Scientific Assessment of Ozone Depletion: 2018,
752  Report No., Global Ozone Research and Monitoring Project, Geneva, Switzerland, 588 pp. pp.,
753  2018.

754  Wong, J. P. S., Carslaw, N., Zhao, R., Zhou, S., and Abbatt, J. P. D.: Observations and impacts
755  of bleach washing on indoor chlorine chemistry, Indoor Air, 27, 1082–1090,
756  https://doi.org/10.1111/ina.12402, 2017.

757  Xu, D., Zhong, W., Deng, L., Chai, Z., and Mao, X.: Levels of Extractable Organohalogens in
758  Pine Needles in China, Environ Sci Technol, 37, 1–6, https://doi.org/10.1021/es025799o, 2003.

759  Xu, D., Tian, Q., and Chai, Z.: Determination of extractable organohalogens in the atmosphere
760  by instrumental neutron activation analysis, J Radioanal Nucl Chem, 270, 5–8,
761  https://doi.org/10.1007/s10967-006-0302-7, 2006.

762  Xu, D., Dan, M., Song, Y., Chai, Z., and Zhuang, G.: Instrumental neutron activation analysis of
763  extractable organohalogens in PM2.5 and PM10 in Beijing, China, J Radioanal Nucl Chem, 271,
764  115–118, https://doi.org/10.1007/s10967-007-0115-3, 2007.

765  Yang, M. and Fleming, Z. L.: Estimation of atmospheric total organic carbon (TOC) – paving the
766  path towards carbon budget closure, Atmos Chem Phys, 19, 459–471,
767  https://doi.org/10.5194/acp-19-459-2019, 2019.

768  Yeung, L. W. Y., Miyake, Y., Taniyasu, S., Wang, Y., Yu, H., So, M. K., Jiang, G., Wu, Y., Li,
769  J., Giesy, J. P., Yamashita, N., and Lam, P. K. S.: Perfluorinated Compounds and Total and

Extractable Organic Fluorine in Human Blood Samples from China, Environ Sci Technol, 42, 8140–8145, https://doi.org/10.1021/es800631n, 2008.

Young, C. J., Washenfelder, R. A., Edwards, P. M., Parrish, D. D., Gilman, J. B., Kuster, W. C., Mielke, L. H., Osthoff, H. D., Tsai, C., Pikelnaya, O., Stutz, J., Veres, P. R., Roberts, J. M., Griffith, S., Dusanter, S., Stevens, P. S., Flynn, J., Grossberg, N., Lefer, B., Holloway, J. S., Peischl, J., Ryerson, T. B., Atlas, E. L., Blake, D. R., and Brown, S. S.: Chlorine as a primary radical: Evaluation of methods to understand its role in initiation of oxidative cycles, Atmos Chem Phys, 14, 3427–3440, https://doi.org/10.5194/acp-14-3427-2014, 2014.

Zhai, S., Wang, X., McConnell, J. R., Geng, L., Cole-Dai, J., Sigl, M., Chellman, N., Sherwen, T., Pound, R., Fujita, K., Hattori, S., Moch, J. M., Zhu, L., Evans, M., Legrand, M., Liu, P., Pasteris, D., Chan, Y.-C., Murray, L. T., and Alexander, B.: Anthropogenic Impacts on Tropospheric Reactive Chlorine Since the Preindustrial, Geophys Res Lett, 48, e2021GL093808, https://doi.org/https://doi.org/10.1029/2021GL093808, 2021.

Zhang, W., Jiao, Y., Zhu, R., Rhew, R. C., Sun, B., and Dai, H.: Chloroform (CHCl3) Emissions From Coastal Antarctic Tundra, Geophys Res Lett, 48, e2021GL093811, https://doi.org/https://doi.org/10.1029/2021GL093811, 2021.